Available online at www.sciencedirect.com
ScienceDirect
Journal of Hazardous Materials 157 (2008) 34–46
Journal of Hazardous Materials
www.elsevier.com/locate/jhazmat

Adsorption isotherm models for dye removal by cationized starch-based material in a single component system: Error analysis

Frédéric Gimbert, Nadia Morin-Crini, François Renault, Pierre-Marie Badot, Grégorio Crini *

University of Franche-Comté, Laboratory of Chrono-Environment, UMR UFC/CNRS 6249, Place Leclerc, 25030 Besançon Cédex, France

Received 1 October 2007; received in revised form 18 December 2007; accepted 19 December 2007
Available online 26 December 2007

Abstract

This article describes the adsorption of an anionic dye, namely C.I. Acid Blue 25 (AB 25), from aqueous solutions onto a cationized starch-based adsorbent. Temperature was varied to investigate its effect on the adsorption capacity. Equilibrium adsorption isotherms were measured for the single component system and the experimental data were analyzed by using Langmuir, Freundlich, Tempkin, Generalized, Redlich–Peterson, and Toth isotherm equations. Five error functions were used to determine the alternative single component parameters by non-linear regression due to the bias in using the correlation coefficient resulting from linearization. The error analysis showed that, compared with other models, the Langmuir model described best the dye adsorption data. Both linear regression method and non-linear error functions provided the best-fit to experimental data with the Langmuir model.

Keywords: Adsorption; Starch; Acid Blue 25; Isotherm; Langmuir; Freundlich; Tempkin; Generalized model; Redlich–Peterson; Toth; Error analysis

1. Introduction

The removal of dye molecules from wastewaters is a matter of great interest in the field of water pollution. Several physical, chemical and biological decolorization methods [1–3] such as coagulation/flocculation treatment, biodegradation processes, oxidation methods, membrane filtration, and adsorption have been reported and attempted for the removal of dyes from plastics, dyestuffs, pulp and paper, and textile effluents. Among these numerous techniques of dye removal, it is now recognized that adsorption using solid adsorbents is an effective and useful process [4–6]. Conventional materials such as commercial activated carbons and organic resins have been used with success. However, their widespread use is restricted due to high cost. For this reason, alternative non-conventional materials including natural materials (clays, siliceous materials, zeolites), waste materials from agriculture and industry (by-products), and biosorbents (peat, biomasses, polysaccharides) have been proposed and studied for their ability to remove dyes [7,8]. Recently, Crini [9] reported an extensive list of non-conventional adsorbent literature for dye removal and discussed their advantages and drawbacks. Polysaccharides such as chitin and starch, and their derivatives (chitosan, cyclodextrins) deserve particular attention [10–12]. These biopolymers represent an interesting and attractive alternative as adsorbents because of their low-cost, particular polymeric structure, physical and chemical properties, and excellent adsorption properties towards a wide range of pollutants, resulting from the presence of chemical reactive groups in polymer chains [12].

The first major challenge for the adsorption field is to select the most promising types of adsorbent, mainly in terms of high capacity and adsorption rate, high selectivity, and low-cost [8,12]. The next real challenge is to identify clearly the adsorption mechanism(s), in particular the interactions which are implicated at the adsorbent/adsorbate interface. Adsorption properties and equilibrium data, commonly known as adsorp-

* Corresponding author. Tel.: +33 3 81 66 57 01; fax: +33 3 81 66 57 97.
E-mail address: gregorio.crini@univ-fcomte.fr (G. Crini).

0304-3894/$ – see front matter © 2007 Elsevier B.V. All rights reserved.
doi:10.1016/j.jhazmat.2007.12.072

Nomenclature

a_L	Langmuir isotherm constant ($l\,mg^{-1}$)
A	Temkin isotherm constant ($l\,g^{-1}$)
B	Temkin isotherm constant
C_e	liquid phase dye concentration at equilibrium ($mg\,l^{-1}$)
C_o	initial dye concentration in liquid phase ($mg\,l^{-1}$)
K	saturation constant (mg/l)
K_F	Freundlich constant ($l\,g^{-1}$)
K_L	Langmuir isotherm constant ($l\,g^{-1}$)
q_e	amount of dye adsorbed at equilibrium ($mg\,g^{-1}$)
q_t	amount of dye adsorbed at time t ($mg\,g^{-1}$)
q_{max}	maximum adsorption capacity of the adsorbent ($mg\,g^{-1}$)
m	mass of adsorbent used (g)
n	cooperative binding constant
n_F	Freundlich isotherm exponent
R^2	linear regression coefficient of determination
t	time (min)
t_e	equilibrium time (min)
T	temperature (K)
V	volume of dye solution (l)
x	amount of dye adsorbed (mg)

tion isotherms, describe how pollutants interact with adsorbent materials and are thus critical in optimizing the use of adsorbents [8,13]. In order to optimize the design of an adsorption system to remove dye from solutions, it is important to establish the most appropriate correlation for the equilibrium curve. An accurate mathematical description of equilibrium adsorption capacity is indispensable for reliable prediction of adsorption parameters and quantitative comparison of adsorption behavior for different adsorbent systems (or for varied experimental conditions) within any given systems [13–15].

There are several isotherm models available for analysing experimental data and for describing the equilibrium of adsorption, including Langmuir, Freundlich, BET, Toth, Tempkin, Redlich–Peterson, Sips, Frumkin, Harkins–Jura, Halsey, Henderson and Dubinin–Radushkevich isotherms [13–15]. Various researchers have used these isotherms to examine the importance of different factors on dye molecule adsorption by a given adsorbent. However, the two most frequently used equations applied in solid/liquid systems to describe adsorption isotherms are the Langmuir [16] and the Freundlich [17] models and the most popular isotherm theory [18] is the Langmuir model which is commonly used for the adsorption of dyes onto biopolymers, although these models were initially developed for the modelling of the adsorption of gas solutes onto metallic surfaces, and are based on the hypothesis of physical adsorption.

There is no doubt that mathematical modelling is an invaluable tool for the analysis and design of adsorption systems and also for the theoretical evaluation and interpretation of thermodynamic parameters. However, an isotherm may fit experimental data accurately under one set of conditions but fail entirely under another. In addition, no single model has been found to be generally applicable [14]. This is readily understandable in the light of the hypotheses associated with their respective deviations. In single-component isotherm studies, the optimization procedure requires an error function to be defined in order to quantitatively compare the applicability of different models in fitting data. To determine isotherm constants for two-parameter isotherms such as the Langmuir and the Freundlich models, two methods are available: (i) the non-linear method consists in fitting the isotherm equation to the data in its non-linear form and (ii) the linear method is based on converting the equation into a linear form by transforming the isotherm variables [13,14,19,20]. In the literature, linear regression is the most commonly used method to estimate adsorption, and linear coefficients of determination are preferred. However, the use of this method is limited to solving linear forms of equation which measure the difference between experimental data and theoretical data in linear plots only, but not the errors in isotherm curves. Several studies have shown that the linearization of a non-linear isotherm expression produces different outcomes [19–22]. Porter et al. [19] showed that the values of individual isotherm constants changed with the error methodology selected. They obtained contradicting results from linearization by using different error functions. Ho [20] also pointed out that the non-linear method was a better way to obtain the isotherm parameters. Recently, similar observations have also been reported by Allen et al. [21] and Wong et al. [22]. Ho et al. [23], Tor and Cengeloglu [24], and Crini et al. [25] reported that linear regression and the non-linear Chi-square analysis gave different models as the best-fitting isotherm for the given data set, thus indicating a significant difference between the analytical methods. These authors showed that the non-linear Chi-square test provided a better determination for the experimental data, in agreement with the previous work published by Ho [20].

In our group, we have recently patented a new cationized starch-based material [26]. This non-conventional low-cost material was prepared from a solid agro-food by-product originating in significant amounts in industrial processes, namely a starch-enriched flour. This flour is one of the cheapest and most unconventional materials and its utilization for the treatment of wastewater from another industry could be helpful not only to the environment in solving the solid waste disposal problem, but also to the economy. In addition, the adsorbent is also regarded as environmentally friendly and substantially less expensive than commercial activated carbons and synthetic commercial adsorbents prepared by using petroleum-based raw materials.

In this paper, we describe the adsorption of C.I. Acid Blue 25 (AB 25) from aqueous solutions onto this cationized adsorbent. Equilibrium adsorption isotherms were measured for the single component system and the experimental data were analyzed thanks to six commonly used models, namely the Langmuir, Freundlich, Tempkin, Generalized, Redlich–Peterson, and Toth isotherm equations. A detailed error analysis was undertaken to investigate the effect of using different error criteria for the determination of the single component isotherm parameters and thus obtain the best-fit isotherm and isotherm parameters which

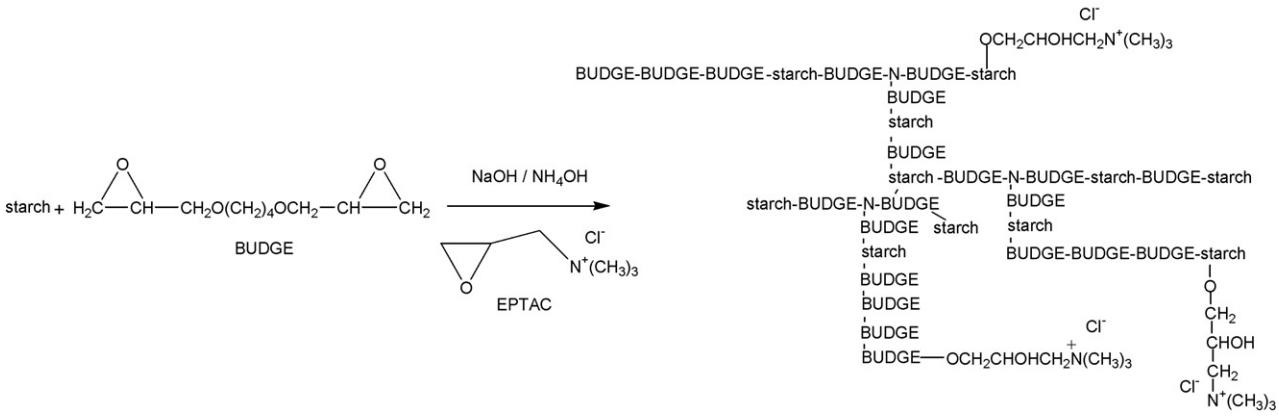

Scheme 1. Synthesis of cationized-starch-based material.

describe the adsorption process. Five different error functions were used, i.e. the sum of the squares of the errors (ERRSQ), the hybrid fractional error function (HYBRID), the Marquardt's percent standard deviation (MPSD), the average relative error (ARE) and the sum of the absolute errors (EABS). These error functions were evaluated and minimized in each case across the respective data. The sum of normalized errors (SNE) was used to select the optimum isotherm parameters among the set of isotherm parameters provided by the minimization of each error function. This normalization procedure allows a direct combination of these scaled errors and identifies the optimum parameter set by its minimum SNE values [19].

2. Materials and methods

2.1. Adsorbent

The adsorbent was prepared in one step by reticulation of a starch-enriched flour thanks to 1,4-butanediol diglycidylether (BUDGE) as crosslinking agent in the presence of NH_4OH and 2,3-epoxy-propyltrimethylammonium chloride (EPTAC) (Scheme 1) [26]. During the crosslinking step with BUDGE, polymer chains were cationized with EPTAC. The polymer characteristics have been reported in Table 1.

2.2. Adsorbate

The adsorption capacity was investigated by using C.I. Acid Blue 25 (AB 25) as model guest solute. AB 25 was purchased from Aldrich (Saint Quentin en Fallavier, France) and was used as received (see Table 2 for its characteristics). AB 25 was chosen because of its known strong adsorption onto solids and it often serves as a model compound for removing organic contaminants from aqueous solutions.

Table 1
Characteristics of ion-exchanger starch material

Particle size	150–250 μm
BET specific surface area	75 $m^2\ g^{-1}$
Swelling capacity	6 ml g^{-1}
N	4%
Degree of substitution (quaternary ammonium groups)	0.81
Zeta potential	Positive values (pH range 3–9)
Water loss at 125 °C	6%

2.3. Adsorption experiments

An accurately weighed quantity of the dye was dissolved in double-distilled water to prepare a stock solution (1000 mg l^{-1}) and the solutions for equilibrium tests were prepared from the stock solution to the desired concentrations through successive dilutions. The calculated concentrations take the dye purity into account. The experiments we conducted used the batch method at natural pH (pH 6 for double-distilled water), previously described in detail [25]. In each experiment, 100 mg of polymer were mixed with 100 ml of an aqueous dye solution at a known concentration in a tightly closed flask. The solution was stirred on a thermostatic mechanical shaker operating at a constant agitation speed; 1 h was found to be enough to reach adsorption equilibrium. The solution was then centrifuged to remove any adsorbent particles, and the supernatant was analyzed for the final dye concentration. Temperature was varied to investigate its effect on the adsorption capacity; isotherm data

Table 2
Dye characteristics

Supplier	Aldrich
C.I. name	Acid Blue 25
C.I. number	62055
Abbreviation	AB 25
Chemical class	Anthraquinone
Dye content (%)	45%
Molecular weight	416.39 g mol^{-1}
Molecular formulae	$C_{20}H_{13}N_2NaO_5S$
λ (nm)	602 nm
Chemical structure	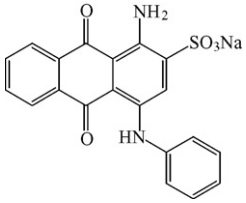

were obtained at 25, 35, 45 and 55 °C in a constant temperature shaker bath which controlled the temperature to within ±1 °C. Each experiment was conducted in triplicate under identical conditions to confirm the results, and was found reproducible (experimental error within 3%). Blanks containing no dye or adsorbent were conducted in similar conditions as controls to evaluate possible color change and/or precipitation processes for both components. The amount of dye adsorbed at equilibrium time (t_e) by the adsorbent (q_e) was calculated from the mass balance equation given by Eq. (1) where C_o and C_e are the initial and final dye concentrations in liquid phase (mg l^{-1}), respectively, V is the volume of dye solution (l) and m the mass of adsorbent used (g).

$$q_e = \frac{V(C_o - C_e)}{m} \quad (1)$$

3. Theory

3.1. Single-component isotherms

Adsorption properties and equilibrium data, commonly known as adsorption isotherms, describe how dye molecules interact with adsorbent materials, and so are critical in optimizing the use of adsorbents. In order to optimize the design of an adsorption system to remove dye from solutions, it is important to establish the most appropriate correlation for the equilibrium curve. An equilibrium is established when the amount of dye being adsorbed onto the adsorbent is equal to the amount being desorbed. The equilibrium solution concentration remains constant. Plotting solid-phase concentration against liquid-phase concentration graphically depicts the equilibrium adsorption isotherm. Several adsorption equilibrium theories available in the literature such as Langmuir, Freundlich, Tempkin, Generalized, Redlich–Peterson, and Toth models (see Table 3 for the equations) can be used to describe equilibrium studies. In this study, experimental data were compared by using these six well-known and widely applied isotherm equations in order to find the best-fitted model for the data obtained. The different equation parameters and the underlying thermodynamic hypotheses of these models often provide insight into both the adsorption mechanism, the surface properties and affinity of the adsorbent [13–15].

3.2. Error functions

The typical assessment of the quality of the isotherm fit to the experimental data is based on the magnitude of the correlation coefficient for the regression, i.e. the isotherm giving an R^2 value closest to unity is deemed to provide the best fit. Linearization using such data transformations implicitly alters the error structure however, and may also violate the error equality of variance (homoscadasticity) and normality hypotheses for standard least squares [31,32]. This may help to explain earlier observations according to which isotherm parameters derived from the linearized forms of the equations are biased in that the Freundlich parameters produce isotherms which tend to fit the data better at low concentrations whereas those derived for the Langmuir isotherm tend to fit the data better at higher concentrations [33].

As an alternative to the linear transformation, non-linear optimization has also been applied to determine isotherm parameter values [19,34,35]; it most commonly uses algorithms based on the Levenberg–Marquardt or Gauss–Newton methods [36,37]. The optimization procedure requires an error function to be defined in order to enable the optimization process to determine and evaluate the fit of the isotherm to the experimental equilibrium data. In this study, five different error functions were examined, and in each case the isotherm parameters were determined by minimising the respective error function across the concentration range studied when using the *solver* add-in with Microsoft's spreadsheet, Excel (Microsoft Corporation, 1994). The error functions studied were as follows.

1. *The sum of the squares of the errors* (ERRSQ) (Eq. (8)): Although this is the most common error function in use, it has one major drawback. Isotherm parameters derived when using this error function will provide a better fit as the magnitude of the errors and thus the squares of the errors increase—biasing the fit towards the data obtained at the high end of the concentration range.

$$\sum_{i=1}^{p}(q_{e,calc} - q_{e,meas})_i^2 \quad (8)$$

2. *The hybrid fractional error function* (HYBRID) (Eq. (9)): This error function was developed by Porter et al. [19] in an attempt to improve the fit of the ERRSQ method at low concentrations. Each ERRSQ value was divided by the experimentally measured q value. In addition, the number

Table 3
The six isotherm models used in this study

Isotherms	Equation	Non-linear equation	Linear equation	Reference
Langmuir	(2)	$q_e = \frac{x}{m} = \frac{K_L C_e}{1+a_L C_e}$	$\frac{C_e}{q_e} = \frac{1}{K_L} + \frac{a_L}{K_L} C_e$	[16]
Freundlich	(3)	$q_e = K_F C_e^{1/n_F}$	$\ln q_e = \ln K_F + \frac{1}{n_F} \ln C_e$	[17]
Tempkin	(4)	$q_e = \frac{RT}{b}(\ln AC_e)$	$q_e = \left(\frac{RT}{b}\right) \ln A + \left(\frac{RT}{b}\right) \ln C_e$	[27]
Generalized	(5)	$q_e = q_{max} \frac{C_e^n}{K+C_e^n}$	$\ln\left[\frac{q_{max}}{q_e} - 1\right] = \ln K - n \ln C_e$	[28]
Toth	(6)	$q_e = \frac{K_T C_e}{[a_T + C_e{}^t]^{1/t}}$	$\ln\left[\frac{q_e}{K_T}\right] = \ln C_e - \frac{1}{t} \ln(a_T + C^t)$	[29]
Redlich–Peterson	(7)	$q_e = \frac{K_R C_e}{1+a_R C_e^\beta}$	$\ln\left[\frac{K_R C_e}{q_e} - 1\right] = \ln a_R + \beta \ln C_e$	[30]

of degrees of freedom of the system – the number of data points, p, minus the number of parameters, n, of the isotherm equation – was included as a divisor.

$$\frac{100}{p-n}\sum_{i=1}^{p}\left[\frac{(q_{e,meas}-q_{e,calc})^2}{q_{e,meas}}\right]_i \quad (9)$$

3. *Marquardt's percent standard deviation* (MPSD) [38] (Eq. (10)): This error function was used previously by a number of researchers in the field [34,39]. It is similar to a geometric mean error distribution that has been modified to allow for the number of degrees of freedom in the system.

$$100\left(\sqrt{\frac{1}{p-n}\sum_{i=1}^{p}\left[\frac{(q_{e,meas}-q_{e,calc})}{q_{e,meas}}\right]_i^2}\right) \quad (10)$$

4. *The average relative error* (ARE) [40] (Eq. (11)): This error function attempts to minimize the fractional error distribution across the entire concentration range.

$$\frac{100}{p}\sum_{i=1}^{p}\left|\frac{(q_{e,calc}-q_{e,meas})}{q_{e,meas}}\right|_i \quad (11)$$

5. *The sum of the absolute errors* (EABS) (Eq. (12)): This approach is similar to the ERRSQ method. Isotherm parameters determined by using this error function will provide a better fit as the magnitude of the errors increase, biasing the fit towards the high concentration data.

$$\sum_{i=1}^{p}\left|q_{e,calc}-q_{e,meas}\right|_i \quad (12)$$

In all the error functions, it is assumed that both the liquid-phase concentration and the solid-phase concentration contribute equally to weighting the error criterion for the model solution procedure. Experimental investigations were undertaken at m/V ratios of 1 g l^{-1}. As a result, the difference in the solid-phase concentrations reflects the difference in the predicted concentrations for both phases.

4. Results and discussion

4.1. The influence of dye concentration and temperature on adsorption capacity

Adsorption equilibrium is established when the amount of dye being adsorbed onto the adsorbent is equal to the amount being desorbed. It is then possible to depict the equilibrium adsorption isotherms by plotting the concentration of the dye in the solid phase versus that in the liquid phase. The distribution of dye molecules between the liquid phase and the biosorbent is a measure of the equilibrium position in the adsorption process and can generally be expressed by one or more of a series of isotherm models [13–15]. The shape of an isotherm may be considered with a view to predicting if a adsorption system is "favorable" or "unfavorable" (see below). The isotherm shape can also provide qualitative information on the nature of the solute–surface interaction. In addition, adsorption isotherms are developed to evaluate the capacity of a material for the adsorption of a particular dye molecule. They constitute the first experimental information which is generally used as a convenient tool to discriminate among different materials and thereby choose the most appropriate for a particular application in given conditions. The most popular classification of adsorption isotherms of solutes from aqueous solutions has been proposed by Giles et al. [41]. Four characteristic classes are identified, based on the configuration of the initial part of the isotherm (i.e., class S, L, H, C). The subgroups relate to the behavior at higher concentrations. The Langmuir class (L) is the most widespread in the case of adsorption of dye compounds from water, and it is characterized by an initial region, which is concave to the concentration axis. Type L also suggests that there is no strong competition between the adsorbate and the solvent to occupy the adsorption sites. However, the H class (high affinity) results from extremely strong adsorption at very low concentrations giving rise to an apparent intercept on the ordinate. The H-type isotherms suggest that the uptake of pollutants by materials is associated with chemical forces rather than with physical attractions.

Fig. 1 shows the equilibrium adsorption of AB 25 (q_e versus C_e) when using a cationized starch-based material for different temperatures. The shape of the isotherms indicates L-behavior according to Giles et al. [41] classification, confirming high affinity between the adsorbent surface and the dye molecules. It was shown that the equilibrium uptake increased with the increase in initial dye concentrations in the range of experimental concentration used. Each isotherm (experimental points) rises sharply in the initial stages for low C_e and q_e values, thus indicating that there are plenty of readily accessible sites and a great affinity of the material for the dye molecules. The adsorbent is saturated when the plateau is reached. The decrease in the slope of the isotherm, tending to a monolayer, considerably increasing the C_e values for a small increase in q_e, is due to the less active sites being available at the end of the adsorption process. It was clear that the polymer had a considerable affinity for the anionic dye with an approximate monolayer saturation capacity of 300 mg g^{-1}. The adsorption mechanism was a

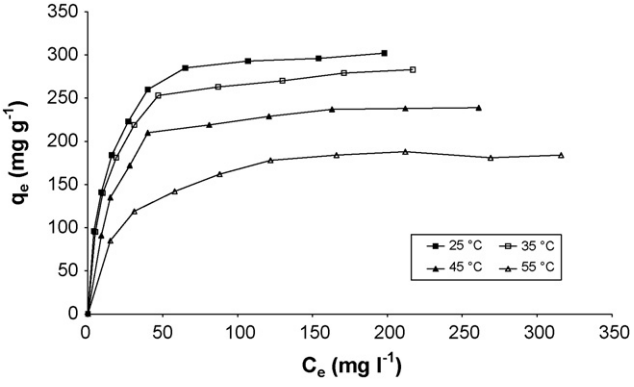

Fig. 1. Adsorption isotherm for AB 25 by a cationized starch-based adsorbent at four different temperatures (*conditions*: contact time = 1 h; volume = 100 ml; material mass = 100 mg; pH 6).

multi-step process involving adsorption on the external surface, diffusion into the polymer network and electrostatic interactions between the sulfonate groups of the dye molecules and the quaternary ammonium groups present at the surface of the material (submitted work). In other research studies [12,25], we demonstrated that this kind of polymer possesses a remarkably high swelling capacity in water due to the hydrophilic nature of its crosslinked units and, consequently, its network is sufficiently expanded to allow a fast diffusion process for the dye molecules. The rapid and extensive uptake with liquid concentration by the polymer, followed by a tailing off in the isotherm with an apparent monolayer being achieved, suggests that the Langmuir isotherm should provide a reasonable description and analysis of the data.

However, it was also shown that the adsorption capacity decreased with increasing temperature, thus indicating that the adsorption of AB 25 onto material was exothermic in nature. It is well known that temperature plays an important role in adsorption by biopolymers, with generally a negative influence on the amount adsorbed. Similar results were reported by Abdel-Aal et al. [42], Xu et al. [43], and Baouab et al. [44].

4.2. The Langmuir model

The Langmuir adsorption isotherm [16] is most widely used for the adsorption of a pollutant from a liquid solution given the following hypotheses:

- monolayer adsorption (the adsorbed layer is one molecule thick);
- adsorption takes place at specific homogeneous sites within the adsorbent;
- once a dye occupies a site, no further adsorption can take place at that site;
- adsorptional energy is constant and does not depend on the degree of occupation of an adsorbent's active centres;
- the strength of the intermolecular attractive forces is believed to fall off rapidly with distance;
- the adsorbent has a finite capacity for the dye (at equilibrium, a saturation point is reached where no further adsorption can occur);
- all sites are identical and energetically equivalent;
- the adsorbent is structurally homogeneous;
- there is no interaction between molecules adsorbed on neighboring sites.

The Langmuir equation is represented by Eq. (2) (Table 3) where x is the amount of dye adsorbed (mg); m is the amount of adsorbent used (g); C_e (mg L^{-1}) and q_e (mg g^{-1}) are the liquid phase concentration and solid phase concentration of adsorbate at equilibrium, respectively; K_L (L g^{-1}) and a_L (L mg^{-1}) are the Langmuir isotherm constants. The Langmuir isotherm constants, K_L and a_L are evaluated through linearization of Eq. (2). By plotting C_e/q_e against C_e, it is possible to obtain the value of K_L from the intercept which is $1/K_L$ and the value of a_L from the slope which is a_L/K_L.

4.3. The Freundlich model

The Freundlich equilibrium isotherm equation [17] was also used to describe experimental adsorption data. This isotherm (Eq. (3)) is an empirical equation which is used for the description of multilayer adsorption with interaction between adsorbed molecules. The model predicts that the dye concentrations on the material will increase as long as there is an increase of the dye concentration in the solution (this is not restricted to the monolayer in the adsorbent). The model applies to adsorption onto heterogeneous surfaces with a uniform energy distribution and reversible adsorption. The Freundlich isotherm is the earliest known relationship describing the adsorption equation. The application of the Freundlich equation suggests that adsorption energy exponentially decreases on completion of the adsorptional centres of an adsorbent. This isotherm is expressed by Eq. (3) (see Table 3) where C_e (mg L^{-1}) and q_e (mg g^{-1}) are the liquid phase concentration and solid phase concentration of adsorbate at equilibrium, respectively; K_F is the Freundlich constant (L^{-1} mg) and $1/n_F$ is the heterogeneity factor. The Freundlich constants are empirical constants which depend on several environmental factors. The value of $1/n_F$ ranges between 0 and 1, and indicates the degree of non-linearity between solution concentration and adsorption as follows [45]: if the value of $1/n_F$ is equal to unity, the adsorption is linear; if the value is below unity, this implies that the adsorption process is chemical; if the value is above unity, adsorption is a favorable physical process; the more heterogeneous the surface, the closer $1/n_F$ value is to 0 [14].

4.4. The Tempkin model

Tempkin and Pyzhev [27] considered the effects of some indirect adsorbate/adsorbate interactions on adsorption isotherms. They suggested that, because of these interactions and ignoring very low and very large values of concentration, the heat of adsorption of all molecules in the layer would decrease linearly with coverage. In Eq. (4), A and $RT/b = B$ are the Tempkin isotherm constants. Constant B is related to the heat of adsorption.

4.5. The Generalized model

In the Generalized equation (Eq. (5)), K represents the saturation constant (mg L^{-1}); n is the cooperative binding constant; q_{max} is the maximum adsorption capacity of the adsorbent (mg g^{-1}); for each temperature, its value is calculated using the K_L/a_L ratio obtained from the Langmuir model; q_e (mg g^{-1}) and C_e (mg L^{-1}) are the equilibrium adsorbate concentrations in the solid and liquid phase, respectively. A plot of the equilibrium data in the form of $\ln[(q_{max}/q_e) - 1]$ versus $\ln C_e$ gives K and n constants [28].

4.6. The Toth model

The Toth model [29] is derived from potential theory and is applicable to heterogeneous adsorption. This isotherm (Eq. (6))

Table 4
Langmuir isotherm constants with error analysis

	Linear transform (LTFM)	Sum of the squares of the errors (ERRSQ)	Hybrid fractional error (HYBRID)	Marquardt's percentage standard deviation (MPSD)	Average relative error (ARE)	Sum of the absolute errors (EABS)
25 °C						
K_L (L g^{-1})	31.456	29.405	30.017	31.009	28.060	28.050
a_L (L mg^{-1})	0.099	0.091	0.094	0.098	0.088	0.088
R^2 (linear)	0.999					
ERRSQ	411.377	**376.182**	383.662	433.213	506.942	503.477
HYBRID	**14.445**	15.727	15.423	16.263	21.398	21.327
MPSD	**2.753**	3.372	3.241	3.159	4.039	4.038
ARE	**1.467**	1.803	1.810	1.829	1.667	1.664
EABS	49.301	52.549	53.116	54.689	47.728	47.562
SNE	**3.872**	4.258	4.241	4.397	4.806	4.769
35 °C						
K_L (L g^{-1})	27.362	26.852	26.901	27.107	26.860	26.458
a_L (L mg^{-1})	0.092	0.090	0.090	0.091	0.090	0.089
R^2 (linear)	0.999					
ERRSQ	226.616	**223.493**	223.665	225.944	224.812	230.243
HYBRID	7.161	7.141	**7.136**	7.184	7.156	7.418
MPSD	**1.810**	1.854	1.849	1.841	1.853	1.929
ARE	**0.803**	0.801	0.885	0.878	0.865	0.872
EABS	27.869	28.979	28.354	28.370	27.584	**27.396**
SNE	**4.741**	4.894	4.853	4.858	4.814	4.913
45 °C						
K_L (L g^{-1})	20.412	18.978	17.991	17.182	18.959	19.187
a_L (L mg^{-1})	0.081	0.074	0.070	0.066	0.075	0.076
R^2 (linear)	0.999					
ERRSQ	**333.977**	504.970	533.709	606.906	518.924	518.997
HYBRID	**11.576**	22.920	21.359	22.533	23.119	23.800
MPSD	**2.382**	4.161	3.711	3.580	4.130	4.257
ARE	**0.910**	1.642	1.697	1.853	1.562	1.575
EABS	**28.728**	40.693	45.309	52.608	38.292	38.063
SNE	**2.633**	4.432	4.426	4.516	4.367	4.429
55 °C						
K_L (L g^{-1})	10.883	9.527	9.558	9.617	9.890	9.980
a_L (L mg^{-1})	0.055	0.047	0.048	0.048	0.050	0.050
R^2 (linear)	0.998					
ERRSQ	239.83	**182.091**	182.302	183.347	194.937	194.947
HYBRID	10.719	7.592	**7.583**	7.603	8.057	8.057
MPSD	2.628	2.128	2.123	**2.120**	2.174	2.174
ARE	1.558	1.334	1.325	1.314	**1.271**	1.271
EABS	40.186	35.278	35.153	35.011	34.609	**34.609**
SNE	5.000	4.012	4.002	**3.996**	4.070	4.070

Values in bold represent minimum error values and minimum sum of normalized errors (SNE).

presupposes a quasi-Gaussian energy distribution. Most sites have an adsorption energy lower than the peak or maximum adsorption energy.

4.7. The Redlich–Peterson model

Redlich and Peterson [30] have proposed an empirical equation incorporating three parameters which may be used to represent adsorption equilibria over a wide concentration range, and can be applied either in homogeneous or heterogeneous systems due to its versatility. The Redlich–Peterson equation is represented by Eq. (7) where K_R and a_R are isotherm constants (L mg^{-1}), and β is an exponent which lies between 0 and 1. This isotherm combines elements from both the Langmuir and Freundlich equations, and the mechanism of adsorption is a hybrid and does not follow ideal monolayer adsorption. The isotherm has a linear dependence on concentration in the numerator and an exponential function in the denominator. Eq. (7) is simplified to a linear isotherm at low surface coverage (for $\beta = 0$, it is simplified to Henry's equation), to the Freundlich isotherm at high adsorbated concentration (K_R and $a_R \gg 1$, $\beta = 1$), and to the Langmuir isotherm when $\beta = 1$.

4.8. Single-component isotherm parameters

The conventional approach to the determination of the isotherm parameters is by linear regression. Examples of the Langmuir, Freundlich, Tempkin, Generalized, Toth, and Redlich–Peterson isotherms using the linear transform model (LTFM) are illustrated in Figs. 2–7. The values of the

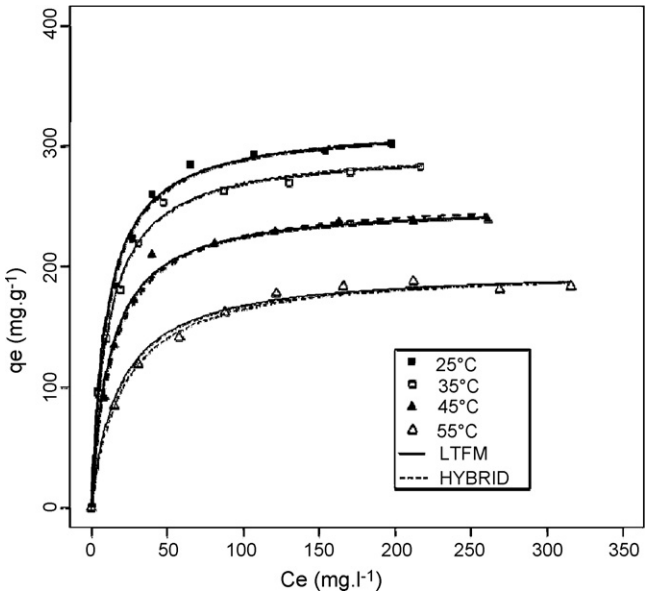

Fig. 2. Single-component Langmuir isotherms and experimental data (*conditions*: contact time = 1 h; volume = 100 ml; material mass = 100 mg; pH 6).

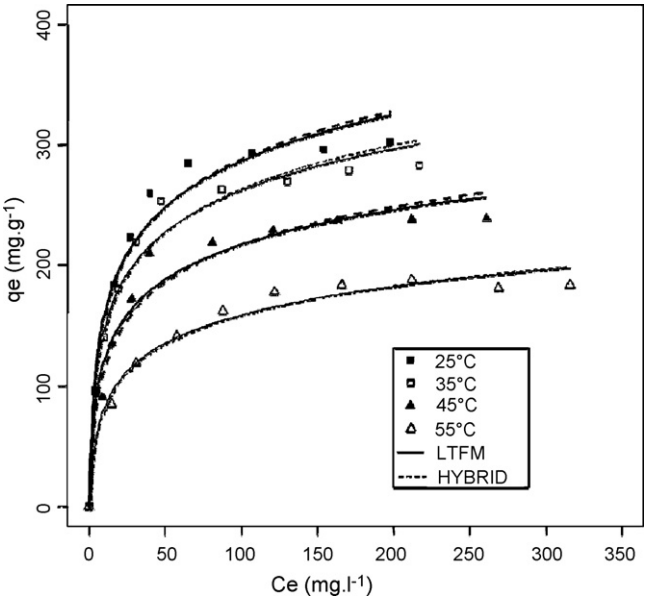

Fig. 4. Single-component Tempkin isotherms and experimental data.

constants for isotherms were obtained from the slope and intercept of the plots of each model linear form. The isotherm parameters obtained, together with the values of the error measures for each isotherm, are all fully presented in Table 4 and the final sum of the normalized error values (SNE) in Tables 5–9.

Examination of the linear isotherm plots suggested that the Langmuir model yielded a much better fit than the other models. In addition, the approach of the isotherm parameters determination by linear regression appears to give acceptable fits to the experimental data with good respective regression coefficients (R^2 values) as shown in the linear transform columns in Tables 5–9. Overall, the Langmuir isotherm has the highest R^2 values (close to unity), whereas the Freundlich and Tempkin values are lower, although the values of $n_F > 1$ indicate favorable adsorption conditions [45]. From Fig. 3, it is also clear that the Langmuir model yields a much better fit than the Freundlich model. Purely from a comparison of the R^2 values, the linearized Langmuir, Toth and Redlich–Peterson isotherms would also be expected to provide a better fit to the experimental data than the linearized Freundlich and Tempkin isotherms. So, the linearized forms of the Langmuir isotherms are found to be linear over the whole concentration range studied, and the correlation coefficients were extremely high, confirming the monolayer coverage of dye onto particles and also the homogeneous distribution of active sites on the material, since the model presupposes that the surface is homogenous. In addi-

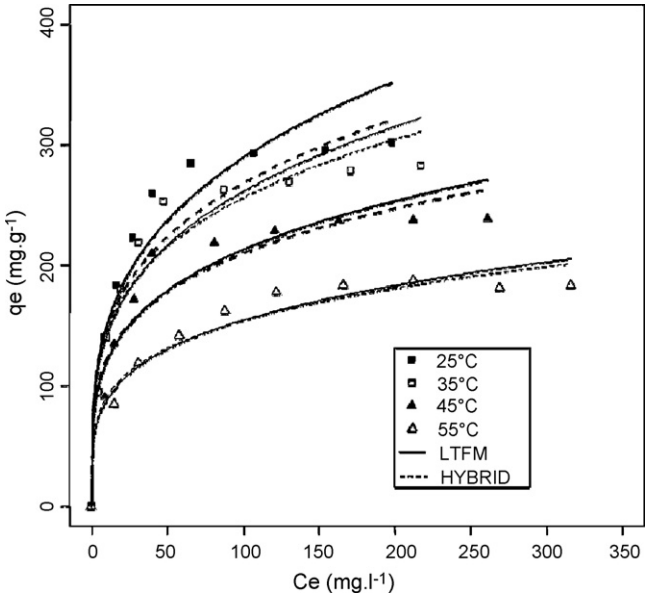

Fig. 3. Single-component Freundlich isotherms and experimental data.

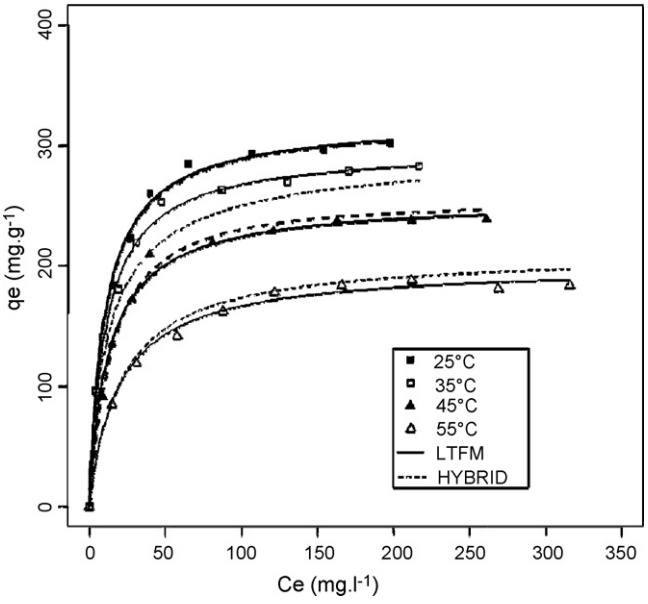

Fig. 5. Single-component Generalized isotherms and experimental data.

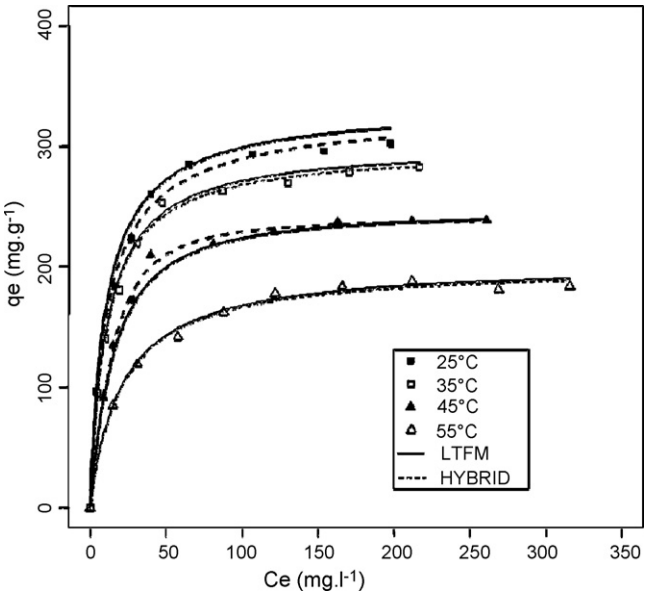

Fig. 6. Single-component Toth isotherms and experimental data.

tion, the general shape of the isotherm curve including sharp curvature near the saturation point and short equilibrium time were highly characteristic of a Langmuir equilibrium with high adsorption capacity. The maximum adsorption capacity of the adsorbent, q_{max}, (equilibrium monolayer capacity or saturation capacity) is numerically equal to K_L/a_L. The q_{max} values were 322, 294, 250 and 196 mg of dye per gram of material for 25, 35, 45, and 55 °C, respectively. The maximum adsorption capacity of AB 25 at 25 °C was comparable to the adsorption capacities of some other adsorbent materials. The q_{max} values also showed that the capacity decreased with increasing temperature. Baouab et al. [44] have reported that the adsorption of organic pollutants onto a solid biopolymer is an exothermic process, and the physical and chemical bonding between the organic molecules

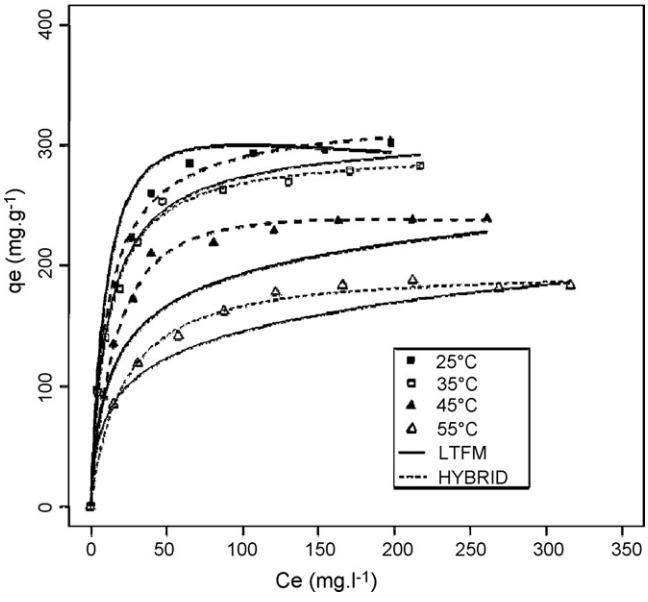

Fig. 7. Single-component Redlich–Peterson isotherms and experimental data.

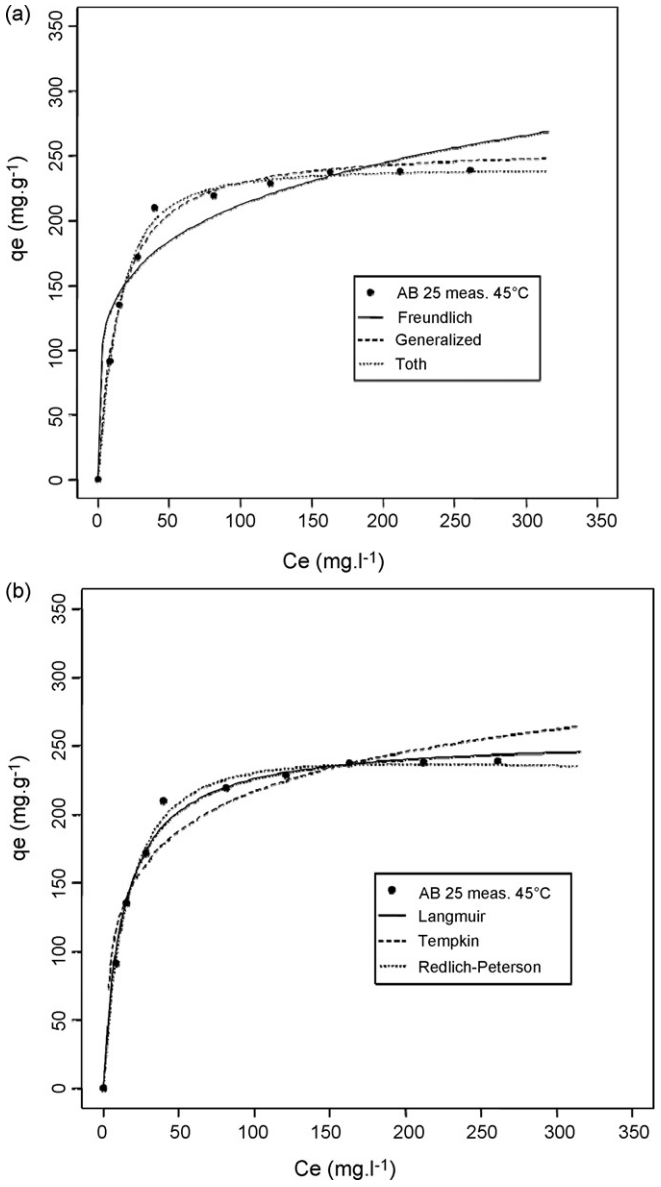

Fig. 8. Comparison of (a) Freundlich, Generalized and Toth isotherms, and (b) Langmuir, Tempkin and Redlich–Peterson isotherms for the adsorption of C.I. Acid Blue 25 onto a cationized starch-based adsorbent.

and the active sites of the material will weaken with increasing temperature. The high degree of correlation for the linearized Langmuir relationship suggested that a single surface reaction with chemisorption was the predominant adsorption step, and possibly the predominant rate-controlling step. Fig. 8 also shows the comparison between the different models at a constant temperature of 45 °C along with the experimental data. Again, it was observed that, in simulation, the equilibrium data were very well represented by the Langmuir isotherm equation when compared with the other equations. There was a good agreement between the experimental value and the calculated value. On the basis of the R^2 values, the order of linear best-fit was Langmuir model > Redlich–Peterson model > Toth model > Generalized model > Tempkin model > Freundlich model at 45 °C. However, it has been shown that this order is temperature-dependant.

Table 5
Freundlich isotherm constants with error analysis

	Linear transform (LTFM)	Sum of the squares of the errors (ERRSQ)	Hybrid fractional error (HYBRID)	Marquardt's percentage standard deviation (MPSD)	Average relative error (ARE)	Sum of the absolute errors (EABS)
25 °C						
K_F (L mg^{-1})	76.925	95.891	84.004	74.892	73.667	95.991
n_F	3.479	4.289	3.809	3.458	3.384	4.261
R^2 (linear)	0.905					
SNE	4.449	4.545	**4.332**	4.566	4.665	4.560
35 °C						
K_F (L mg^{-1})	74.951	92.022	80.803	71.898	89.972	89.993
n_F	3.690	4.499	3.994	3.616	4.429	4.430
R^2 (linear)	0.892					
SNE	4.648	4.546	**4.365**	4.753	4.452	4.453
45 °C						
K_F (L mg^{-1})	66.573	81.897	70.751	61.726	79.886	93.790
n_F	3.965	4.845	4.236	3.780	4.684	5.495
R^2 (linear)	0.833					
SNE	4.154	4.079	**3.959**	4.370	4.037	4.624
55 °C						
K_F (L mg^{-1})	49.074	58.023	52.668	48.322	52.572	58.873
n_F	4.021	4.667	4.292	4.001	4.204	4.614
R^2 (linear)	0.902					
SNE	4.558	4.475	**4.418**	4.646	4.456	4.753

Values in bold represent minimum sum of normalized errors (SNE).

In addition, the value of the Redlich–Peterson exponent being greater than 1 ($\beta > 1$ at 25 °C, see Table 9) suggests that no constraint was fixed to the Redlich–Peterson exponent when using regression techniques. Due to its simplicity compared with the non-linear analysis, linear regression may give an inaccurate conclusion.

Due to the inherent bias resulting from linearization, alternative single-component parameter sets were determined by non-linear regression using the five different error functions as described earlier, namely ERRSQ, HYBRID, MPSD, ARE and EABS. The process of minimizing the respective error functions across the experimental concentration ranges yielded

Table 6
Tempkin isotherm constants with error analysis

	Linear transform (LTFM)	Sum of the squares of the errors (ERRSQ)	Hybrid fractional error (HYBRID)	Marquardt's percentage standard deviation (MPSD)	Average relative error (ARE)	Sum of the absolute errors (EABS)
25 °C						
A (L g^{-1})	1.735	1.735	1.433	1.297	1.250	1.500
B	55.509	55.509	57.946	59.447	59.644	57.699
R^2 (linear)	0.952					
SNE	4.909	4.909	4.591	**4.478**	4.628	4.645
35 °C						
A (L g^{-1})	1.870	1.870	1.448	1.236	1.582	1.584
B	50.042	50.042	52.892	55.043	50.703	50.681
R^2 (linear)	0.947					
SNE	4.781	4.781	**4.493**	4.633	4.639	4.642
45 °C						
A (L g^{-1})	1.804	1.804	1.195	0.905	1.567	1.568
B	41.702	41.702	45.351	48.396	42.758	42.753
R^2 (linear)	0.899					
SNE	4.632	4.632	4.508	4.774	**4.481**	4.481
55 °C						
A (L g^{-1})	1.105	1.105	0.899	0.779	0.855	0.889
B	33.717	33.717	35.162	36.299	36.306	35.889
R^2 (linear)	0.932					
SNE	4.712	4.712	**4.646**	4.706	4.764	4.672

Values in bold represent minimum sum of normalized errors (SNE).

Table 7
Generalized isotherm constants with error analysis

	Linear transform (LTFM)	Sum of the squares of the errors (ERRSQ)	Hybrid fractional error (HYBRID)	Marquardt's percentage standard deviation (MPSD)	Average relative error (ARE)	Sum of the absolute errors (EABS)
25 °C						
K (mg L^{-1})	9.502	10.576	9.698	8.964	10.181	10.730
n	0.959	0.987	0.956	0.924	0.950	0.966
R^2 (linear)	0.986					
SNE	4.401	4.404	**4.225**	4.337	4.746	4.971
35 °C						
K (mg L^{-1})	10.214	8.204	8.744	9.093	9.123	8.294
n	0.972	0.810	0.828	0.841	0.835	0.805
R^2 (linear)	0.990					
SNE	**2.594**	4.902	4.662	4.715	4.705	4.707
45 °C						
K (mg L^{-1})	11.483	17.598	19.935	21.993	16.976	13.001
n	0.949	1.084	1.121	1.153	1.047	0.983
R^2 (linear)	0.969					
SNE	4.772	3.704	**3.701**	3.823	3.833	4.065
55 °C						
K (mg L^{-1})	18.231	21.685	20.759	19.951	18.948	19.303
n	0.969	1.007	0.995	0.983	0.970	0.977
R^2 (linear)	0.936					
SNE	5.000	4.544	4.490	4.776	4.520	**4.488**

Values in bold represent minimum sum of normalized errors (SNE).

the isotherm constants (Tables 4–9). As shown in these tables, the results tend to suggest that a lower absolute error value is obtained for both Langmuir and Toth isotherms. However, it was noted that only the Langmuir model proved to be efficient for both linear and non-linear methods. Once again, the Freundlich isotherm exhibited a tendency to yield higher error values. The application of the different error functions will provide different sets of isotherm constants, sometimes close to one another

Table 8
Toth isotherm constants with error analysis

	Linear transform (LTFM)	Sum of the squares of the errors (ERRSQ)	Hybrid fractional error (HYBRID)	Marquardt's percentage standard deviation (MPSD)	Average relative error (ARE)	Sum of the absolute errors (EABS)
25 °C						
K_T (mg g^{-1})	336.455	323.281	331.607	341.561	324.061	321.237
a_T (mg L^{-1})	7.497	10.210	7.122	5.396	8.082	10.130
t	0.909	0.980	0.876	0.792	0.909	0.965
R^2 (linear)	0.991					
SNE	4.235	4.164	**3.977**	4.115	4.441	4.757
35 °C						
K_T (mg g^{-1})	302.764	295.103	298.091	301.187	296.853	299.102
a_T (mg L^{-1})	10.008	12.942	10.678	9.179	9.834	9.612
t	0.973	1.045	0.990	0.944	0.977	0.961
R^2 (linear)	0.996					
SNE	3.704	3.955	3.637	3.680	3.761	**3.543**
45 °C						
K_T (mg g^{-1})	247.268	240.424	240.316	240.907	240.061	241.930
a_T (mg L^{-1})	32.137	109.786	112.340	116.638	110.003	110.050
t	1.198	1.571	1.576	1.585	1.562	1.558
R^2 (linear)	0.985					
SNE	5.000	2.343	2.337	2.334	2.376	**2.305**
55 °C						
K_T (mg g^{-1})	203.503	199.007	200.990	202.804	199.978	198.515
a_T (mg L^{-1})	19.856	27.478	21.448	17.841	26.985	26.059
t	0.988	1.063	1.005	0.960	1.052	1.049
R^2 (linear)	0.989					
SNE	4.857	3.639	3.523	**3.491**	3.672	3.623

Values in bold represent minimum sum of normalized errors (SNE).

Table 9
Redlich–Peterson isotherm constants with error analysis

	Linear transform (LTFM)	Sum of the squares of the errors (ERRSQ)	Hybrid fractional error (HYBRID)	Marquardt's percentage standard deviation (MPSD)	Average relative error (ARE)	Sum of the absolute errors (EABS)
25 °C						
K_R (L g^{-1})	30.133	28.142	31.301	34.555	28.265	26.456
a_R (L mg^{-1})	0.055	0.081	0.105	0.134	0.090	0.073
β	1.108	1.014	0.985	0.957	0.997	1.023
R^2 (linear)	0.978					
SNE	5.000	1.837	**1.785**	1.869	1.977	1.958
35 °C						
K_R (L g^{-1})	28.396	25.500	26.569	27.553	28.244	26.778
a_R (L mg^{-1})	0.101	0.079	0.087	0.096	0.099	0.092
β	0.984	1.015	1.005	0.993	0.992	0.997
R^2 (linear)	0.999					
SNE	4.335	1.837	**4.527**	4.530	4.576	4.530
45 °C						
K_R (L g^{-1})	24.600	15.055	14.507	14.080	14.585	14.719
a_R (L mg^{-1})	0.210	0.038	0.034	0.031	0.039	0.040
β	0.874	1.083	1.094	1.105	1.069	1.066
R^2 (linear)	0.990					
SNE	5.000	2.321	**2.314**	2.365	2.337	2.336
55 °C						
K_R (L g^{-1})	26.066	8.532	9.074	9.514	9.752	8.076
a_R (L mg^{-1})	0.395	0.035	0.041	0.046	0.047	0.029
β	0.816	1.035	1.018	1.004	1.009	1.060
R^2 (linear)	0.995					
SNE	4.065	3.381	**3.330**	3.362	3.590	3.593

Values in bold represent minimum sum of normalized errors (SNE).

and thus difficult to compare. To identify the optimum or best set of isotherm constants, the results for each set were normalized and combined as a sum of the normalized errors values (SNE) (see for instance [19,35]) presented in Tables 4–9. SNE values were obtained by dividing the error values calculated for each error function for each set of isotherm constants by the maximum errors for that error function. SNE values allowed the comparison between error functions, and the identification of the set of isotherm constants providing the fit closest to the experimental data. For the Freundlich model (Table 5), and for the Redlich–Peterson model too (Table 9), the lowest value of the SNE was obtained by using the HYBRID function irrespective of the temperature. The HYBRID method yielded the best fit in a number of cases. This error function was developed by Porter et al. [19] in order to improve the fit of the ERRSQ method at low concentration values, and it appears to be applicable in this case. For the other models (see, for instance, the Toth isotherm), the validity of any comparison of error functions depends on the temperature. However, the error functions selected in this work provide a reasonably wide selection and the distribution of the experimental data does not give excessive bias to either high or low concentrations.

5. Conclusions

The equilibrium adsorption of C.I. Acid Blue 25 by a cationized starch-based adsorbent has been reported. This material exhibited an interesting sorption capacity although the value was temperature-dependent. The experimental data have been modeled and evaluated by using six different models and six different optimization and error functions. The linear transform model provided the highest R^2 regression coefficient for the case of the Langmuir isotherm. Using any of the error functions for non-linear optimization showed that the Freundlich isotherm was better represented when using the HYBRID error function, which compensated for low concentrations by balancing absolute deviation against fractional error. Also, the Langmuir isotherm yielded the best fit when using the other error functions.

Acknowledgements

The authors thank Brigitte Jolibois and Capucine Robert (Environmental Biology Department, University of Franche-Comté) for assistance during this work, and OSEO/ANVAR and "*Incubateur de Franche-Comté*" for financial support.

References

[1] Y. Anjaneyulu, N. Sreedhara, D. Chary, Suman Raj Samuel, Decolourization of industrial effluents-available methods and emerging technologies—a review, Rev. Environ. Sci. Biotechnol. 4 (2005) 245–273.

[2] H. Singh Rai, M.S. Bhattacharyya, J. Singh, T.K. Bansal, P. Vats, U.C. Banerjee, Removal of dyes from the effluent of textile and dyestuff manufacturing industry: a review of emerging techniques with reference to biological treatment, Crit. Rev. Environ. Sci. Technol. 35 (2005) 219–238.

[3] G. Crini, P.M. Badot, N. Morin-Crini, G. Torri, Wastewater treatment processes: a recent review of the available methods, in: G. Crini, P.M. Badot (coordinators), Traitement et épuration des eaux industrielles polluées (in French), Besançon: Presses Universitaires de Franche-Comté (PUFC), 2007, pp. 15–62 (chapter 1).
[4] G. Thompson, J. Swain, M. Kay, C.F. Forster, The treatment of pulp and paper mill effluent: a review, Bioresour. Technol. 77 (2001) 275–286.
[5] Y. Fu, T. Viraraghavan, Fungal decolorization of dye wastewaters—a review, Bioresour. Technol. 79 (2001) 251–262.
[6] Z. Aksu, Application of biosorption for the removal of organic pollutants: a review, Process Biochem. 40 (2005) 997–1026.
[7] S.J. Allen, B. Koumanova, Decolourisation of water/wastewater using adsorption (Review), J. Univ. Chem. Technol. Metall. 40 (2005) 175–192.
[8] G. McKay, Use of Adsorbents for the Removal of Pollutants from Wastewaters, CRC Press, 1996.
[9] G. Crini, Non-conventional low-cost adsorbents for dye removal: a review, Bioresour. Technol. 97 (2006) 1061–1085.
[10] R. Klimaviciute, A. Riauka, A. Zemaitaitis, The binding of anionic dyes by cross-linked cationic starches, J. Polym. Res. 14 (2007) 67–73.
[11] R.S. Blackburn, Natural polysaccharides and their interactions with dye molecules: applications in effluent treatment, Environ. Sci. Technol. 38 (2004) 4905–4909.
[12] G. Crini, Recent developments in polysaccharide-based materials used as adsorbents in wastewater treatment, Prog. Polym. Sci. 30 (2005) 38–70.
[13] C. Tien, Adsorption Calculations and Modeling, Butterworth-Heinemann Series in Chemical Engineering, Boston, 1994.
[14] B. Al-Duri, in: G. McKay (Ed.), Use of Adsorbents for the Removal of Pollutants from Wastewaters, CRC Press, 1996, pp. 133–173 (chapter 7).
[15] Y.S. Ho, J.F. Porter, G. McKay, Equilibrium isotherm studies for the sorption of divalent metal ions onto peat: copper, nickel and lead single component systems, Water Air Soil Pollut. 141 (2002) 1–33.
[16] I. Langmuir, The constitution and fundamental properties of solids and liquids, J. Am. Chem. Soc. 38 (1916) 2221–2295.
[17] H.M.F. Freundlich, Über die adsorption in lösungen, Z. Phys. Chem. 57 (1906) 385–471.
[18] Y.S. Ho, Removal of copper ions from aqueous solution by tree fern, Water Res. 37 (2003) 2323–2330.
[19] J.F. Porter, G. McKay, K.H. Choy, The prediction of sorption from a binary mixture of acidic dyes using single- and mixed-isotherm variants of the ideal adsorbed solute theory, Chem. Eng. Sci. 54 (1999) 5863–5885.
[20] Y.S. Ho, Selection of optimum sorption isotherm, Carbon 42 (2004) 2115–2116.
[21] S.J. Allen, G. McKay, J.F. Porter, Adsorption isotherm models for basic dye adsorption by peat in single and binary component systems, J. Colloid Int. Sci. 280 (2004) 322–333.
[22] Y.C. Wong, Y.S. Szeto, W.H. Cheung, G. McKay, Adsorption of acid dyes on chitosan-equilibrium isotherm analyses, Proc. Biochem. 39 (2004) 693–702.
[23] Y.S. Ho, W.T. Chiu, C.C. Wang, Regression analysis for the sorption isotherm of basic dyes on sugarcane dust, Bioresour. Technol. 96 (2005) 1285–1291.
[24] A. Tor, Y. Cengeloglu, Removal of congo red from aqueous solution by adsorption onto acid activated red mud, J. Hazard. Mater. B138 (2006) 409–415.
[25] G. Crini, H.N. Peindy, F. Gimbert, C. Robert, Removal of C, I. Basic Green 4 (Malachite Green) from aqueous solutions by adsorption using cyclodextrin-based adsorbent: kinetic and equilibrium studies, Sep. Purif. Technol. 53 (2007) 97–110.
[26] G. Crini, Method for making a gel-type compound for treating effluent, French Patent PCT/FR2006/050549; WO 2006/134299.
[27] M.J. Tempkin, V. Pyzhev, Kinetics of ammonia synthesis on promoted iron catalysts, Acta Physicochim. URSS 12 (1940) 217–256.
[28] F. Kargi, S. Ozmihci, Biosorption performance of powdered activated sludge for removal of different dyestuffs, Enzyme Microbiol. Technol. 35 (2004) 267–271.
[29] J. Toth, State equations of the solid gas interface layer, Acta Chem. Acad. Sci. Hungaria 69 (1971) 311–317.
[30] O. Redlich, D.L. Peterson, A useful adsorption isotherm, J. Phys. Chem. 63 (1959) 1024–1026.
[31] R.H. Myers, Classical and modern regression with applications, PWS-KENT 444–445 (1990) 297–298.
[32] D.A. Ratkowski, Handbook of Nonlinear Regression Models, Marcel Dekker, New York, 1990.
[33] E. Ritcher, W. Schutz, A.L. Myers, Effect of adsorption equation on prediction of multicomponent equilibria by the ideal adsorbed solution theory, Chem. Eng. Sci. 44 (1989) 1609–1616.
[34] A. Seidel-Morgenstern, G. Guiochon, Modelling of the competitive isotherms and the chromatographic separation of two enantiomers, Chem. Eng. Sci. 40 (1993) 215–222.
[35] S.J. Allen, Q. Gan, R. Matthews, P.A. Johnson, Comparison of optimised isotherm models for basic dye adsorption by kudzu, Bioresour. Technol. 88 (2003) 143–152.
[36] T.F. Edgar, D.M. Himmelblau, Optimization of Chemical Processes, McGraw-Hill, New York, 1989, pp. 208–241.
[37] O.T. Hanna, O.C. Sandall, Computational Methods in Chemical Engineering, Prentice-Hall International, Englewood Cliffs, NJ, 1995, pp. 127–130.
[38] D.W. Marquardt, An algorithm for least squares estimation of non-linear parameters, J. Soc. Ind. Appl. Math. 11 (1963) 431–441.
[39] A. Seidel, D. Gelbin, On applying the ideal adsorbed solution theory to multicomponent adsorption equilibria of dissolved organic components on activated carbon, Chem. Eng. Sci. 43 (1988) 79–89.
[40] A. Kapoor, R.T. Yang, Correlation of equilibrium adsorption data of condensable vapours on porous adsorbents, Gas Sep. Purif. 3 (1989) 187–192.
[41] C.H. Giles, D. Smith, A. Huitson, A general treatment and classification of the solute adsorption isotherm I. Theoretical, J. Colloid Int. Sci. 47 (1974) 755–765.
[42] S.E. Abdel-Aal, Y.H. Gad, A.M. Dessouki, Use of rice straw and radiation-modified maize starch/acrylonitrile in the treatment of wastewater, J. Hazard. Mater. B129 (2006) 204–215.
[43] S. Xu, J. Wang, R. Wu, J. Wang, H. Li, Adsorption behaviors of acid and basic dyes on crosslinked amphoteric starch, Chem. Eng. J. 117 (2006) 161–167.
[44] M.H.V. Baouab, R. Gauthier, H. Gauthier, M.E.B. Rammah, Cationized sawdust as ion exchanger for anionic residual dyes, J. Appl. Polym. Sci. 82 (2001) 31–37.
[45] R.E. Treybal, Mass Transfer Operations, McGraw-Hill, New York, 1987.